Scaling of Core Heating Performance for FIREX-I

T. Johzaki[1], H. Nagatomo[1], A. Sunahara[2], H.-B. Cai[3], H. Sakagami[4], K. Mima[1], Y. Nakao[5], H. Nakamura[1], S. Fujioka[1], H. Shiraga[1], H. Azechi[1] and FIREX project group

[1]*Institute of Laser Engineering, Osaka University, Suita, Japan*
[2]*Institute for Laser Technology, Suita, Japan*
[3]*Institute for Applied Physics and Computational Mathematics, Beijing, China*
[4]*National Institute for Fusion Science, Toki, Japan*
[5]*Department of Applied Quantum Physics and Nuclear Engineering, Kyushu University, Fukuoka, Japan*

1. INTRODUCTION

In Institute of Laser Engineering (ILE), Osaka University, a 4-beam bundled new ultra-intense high-energy laser LFEX (Laser for Fast-ignition Experiment) has been constructed, and the Fast-Ignition Realization Experiment Project, Phase-I (FIREX-I) [1] has been started. The final goal of FIREX-I is demonstration of core heating up to 5keV using 10kJ LFEX laser.

The first integrated experiments using LFEX laser have been done, where the LFEX laser was operated with 1-beam and low-energy mode (~500J /1~5ps). About 30-fold enhancement in Y_n was achieved, which is smaller than that in the previous experiments using PW laser (~1000x enhancement) [2]. Compared to the hydro-base core heating simulations, where the energy coupling of heating laser to compressed core $\eta_{L\rightarrow core}$ was numerically given, $\eta_{L\rightarrow core}$ ~20% was expected in the PW experiment, but only $\eta_{L\rightarrow core}$ = 3~5% in the LFEX experiment. One reason for the low $\eta_{L\rightarrow core}$ is the existence of high-level pre-pulse in front of the heating laser. It generates the long-scale low-density plasma (pre- plasma) on the target surface, which leads the fast electron generation point away from the core and generates very energetic fast electrons not contributing to the core heating. As the results, the core heating becomes less efficient.

In the present paper, to understand the core heating physics and to clarify the bottlenecks for achieving high efficiency, we evaluate the core heating performance by separating the heating process into 3 phases; 1) energy coupling from heating laser to fast electrons η_1, 2) fast electron core hitting rate (divergence and tip effects) η_2 and 3) energy deposition rate in the core η_3. The fast electron generation is evaluated using 2D PIC code, and the following processes (transport effect in tip and energy deposition in core) are treated with a simple analytical model.

2. FAST ELECTRON GENERATION

The fast electron generation in a cone is evaluated with 2D PIC simulations. The initial target configuration is shown in **Fig.1**. We assumed the cone open angle of 30 degree, the tip width and thickness of $15\lambda_L$ (λ_L is the laser wavelength) and $5\lambda_L$, the wall thickness of $8\lambda_L$, the electron density of $40n_c$ (n_c is the laser critical density). The ion in the cone is Au with Z=40 and A=197. As for the imploded plasma surrounding the cone, the $40n_c$ fully-ionized CD plasma is located in the outer region of the cone. The simulations were carried out for two cases; 1) no pre-plasma case and 2) the case with 10μm-scale pre-plasma from 3 n_c to $0.01n_c$ in the vacuum region inside of cone. The irradiated laser parameters are 1.06μm wavelength, the Gaussian radial profile with $25\lambda_L$ width, 2.8×10^{19}W/cm^2 peak intensity and the 1ps pulse duration (constant intensity) with the Gaussian rising and damping in 5 laser periods at the beginning and end of pulse. The forward-directed fast electron profile is observed at $x = 65\lambda_L$ in the region of $-10\lambda_L < y < 10\lambda_L$.

The pre-plasma density assumed here is relativistically under-dense for the present intensity. In both cases (with and w/o pre-plasma), thus, the laser pulse can reach the tip and the intensity intensification due to cone focusing can be observed. If the pre-plasma exists, however, the energy conversion of laser to the fast electrons observed at cone tip becomes lower (η_1=72% and 45% for the cases with and w/o pre-plasma) though the higher laser absorption is obtained (86% and 96%, respectively). The fast electrons are generated not only at the tip but also in the pre-plasma if the pre-plasma exists. Some fast electrons generated in the pre-plasma cannot reach the tip, but escape from the cone-side wall, which reduces η_1.

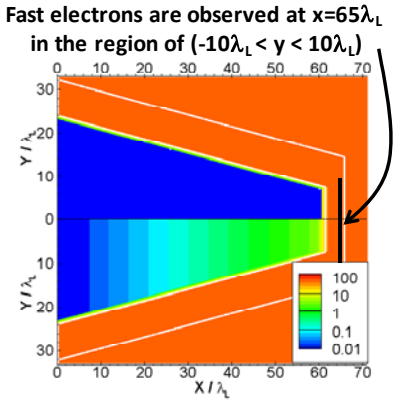

Fig.1 Initial cone configuration. Upper (lower) half for the case w/o pre-plasma (with 10μm scale

Figure 2 shows (a) time- and space-integrated fast electron spectra and (b) time-, space- and energy integrated fast electron angular distributions (normalized by the peak values) measured at the observation region. For the case with pre-plasma, the high energy tail is large compared to the case w/o pre-plasma and the number of low energy electron is reduced, *e.g.*, the energy fractions of low energy component (E<2MeV) to the total fast electron beam are 34% and 11% for the cases w/o and with pre-plasma. (Note that even for the case w/o pre-plasma, the pre-plasma is generated due to the heated plasma expansion from the wall during the heating laser irradiation, which generates the high energy tail.) As for the angular spread, the difference between two cases is small. For the cases with and w/o pre-plasma, the values of full width at half maximum of angular spread are 109 deg. and 99 deg. and the standard deviations, $\sigma_{gen} = \sqrt{\int \left[\theta_{av}^2 - \theta^2 f(\theta)\right] d\theta / \int f(\theta) d\theta}$, are 38deg. and 35deg., respectively, where θ_{av} is the average beam direction defined as $\int \theta \cdot f(\theta) d\theta / \int f(\theta) d\theta$. Such a large angular spread comes from the perturbation at the laser-plasma interaction surface. Due to the interference between laser pulse directly toward the tip and that reflected at the cone wall, the laser-wavelength-scale pulse modulation takes place, which seeds the perturbation at the interaction surface. This perturbation grows during laser irradiation. So, the angular spread of fast electron beam becomes larger during the laser irradiation.

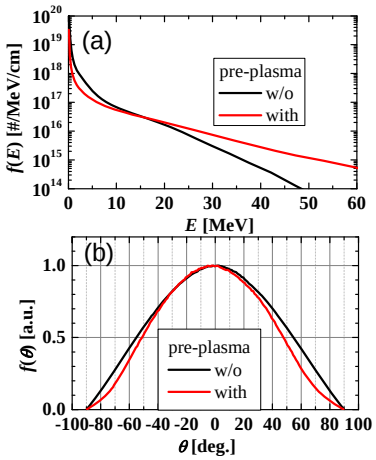

Fig.2 Fast electron profile observed at the tip. (a) time- and space-integrated energy spectra, (b) time-, space- and energy- integrated angular distribution (normalized by the peak values).

In practical, the spectrum has the transverse dependence, $f = f(E, y)$, and the angular spread and the average angle have the energy and transverse dependences, $\sigma_{gen} = \sigma_{gen}(E, y)$ and $\theta_{av} = \theta_{av}(E, y)$. Thus, in the following simple analytical model estimation for core hitting rate η_2 and energy deposition rate in core η_3, we take these dependences into account.

3. CORE HITTING RATE AND ENERGY DEPOSION RATE IN CORE

The Fokker-Planck (or particle) – hydro hybrid simulation is useful for detailed evaluation of fast electron transport and core heating processes. However, a simple analytical model is also valuable for promptly evaluating the core heating performance of generated fast electron beam under the various cone-core conditions. Here, we evaluated the core hitting rate η_2 and energy deposition rate in the core η_3 using simple analytical model without self-generated field effects.

3.1 Core Hitting Rate

The core hitting rate η_2 is defined as the ratio of energy carried by fast electrons into the core after transport in the cone tip and the gap between tip and core to the initial fast electron beam energy (observed at tip in PIC simulations). In the evaluation of η_2, the scattering and energy loss in the tip are included, but neglecting those in the gap. On the basis of the central limiting theorem, the angular distribution of injected beam after multiple scattering can be described by the Gaussian distribution with mean-square angle. We calculated the mean-square angle $< \theta_{tip}^2 > (E)$ for the Coulomb scattering by bulk ion in the different tip materials (solid Au and CH) with different tip thickness Δx_{tip}. The tip temperature is assumed to be 1keV. The energy loss of fast electron having energy E in the tip is also evaluated using the continuous slowing down model, where the bulk electron stopping by short-range binary collision and long-range collective one [3] are considered.

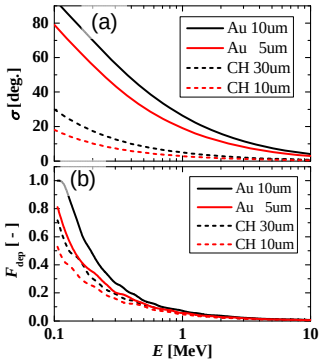

Fig.3 (a) standard deviation of scattering angle $\sigma_{tip}(E)$ and (b) energy loss fraction $F_{dep}(E)$ in tip as a function of E for solid Au and CH tip with different Δx_{tip}.

In **Fig.3**, the standard deviation of scattering angle $\sigma_{tip}(E) = \sqrt{< \theta_{tip}^2 > (E)}$ and the energy loss fraction $F_{dep}(E) = E_{dep}(E)/E$, where $E_{dep}(E)$ is lost energy in tip by fast electron having E, are plotted as a function of E. The Coulomb scattering due to ion is proportion to Z^2, where Z is charge state. Thus, the scattering effect in tip is significant for high-Z Au even if its thickness is much smaller than that for CH tip. Contrary to this, the energy loss depends on $\Delta x_{tip} n_e$ (n_e is the electron number density), so that the material dependence is not so large. From these simple evaluations, the fast electrons with E < 0.2MeV may not contribute to the core heating because of the large scattering angle and energy loss in the tip.

Using the PIC results($f(E, y)$, $\sigma_{gen}(E, y)$ and $\theta_{av}(E, y)$) and the above simple analysis results, we evaluated the core hitting rate η_2. Here, we assumed a CD core with ρR = 0.2g/cm^2, ρ = 100g/cm^3 and R = 20μm, and the distance between tip and core was assumed as D_{tip} = 0 ~ 50μm. The standard deviation of beam angle after tip transport $\sigma_{out}(E, y)$ is evaluated by $\sigma_{out}(E, y) = \sqrt{< \theta_{tip}^2 > (E, y) + < \theta_{tip}^2 > (E)}$, and the fast electron energy after tip transport $E_{out}(E)$ is $E_{out}(E) = E - E_{dep}(E)$. The evaluated η_2 is shown in **Fig.4** for difference cone-core conditions. The distance from the fast electron observation point to the core center D_{tot} is the sum of Δx and D_{tip}. The beam divergence at the generation is so large the dependence of scattering effects on tip material does not appear in η_2 explicitly. On the other hand, due to the large divergence, η_2 strongly depends on D_{tot}. These results indicates that to enhance the η_2, the tip should be located as close to core as possible. A little lower η_2 for the case with pre-plasma is obtained, which is due to larger beam angle θ_{av} at a distance from the center for the case with pre-plasma.

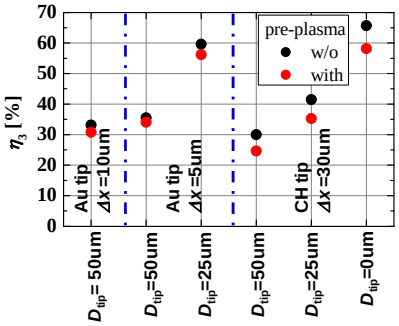

Fig.4 Core hitting rate dependence on cone-core condition.

3.2 Energy Deposition Rate

The energy deposition rate η_3 is evaluated in the same way as that for evaluation of the energy loss in tip. Here we assumed the same core; a CD core with ρ=100g/cm^3 and R = 20μm. Using the

energy spectrum f (E) (time- and space- integrated) obtained in the PIC simulation for the case w/o pre-plasma, the deposited energy $f(E)$x$E_{dep}(E)$ in the core was evaluated and plotted as a function of E in **Fig.5 (a)**, where the black and red lines stand for the evaluation w/o and with the core hitting rate η_2. The contribution ratio, $R_{dep}(E) = \int_0^E f(E)\cdot E_{dep}(E)dE / \int_0^\infty f(E)\cdot E_{dep}(E)dE$ is plotted in **Fig.5(b)**. The present evaluation is for FIREX-I, so the core size is smaller than that required for ignition. Thus, the fast electrons with E>1MeV does not stop in the core, and the heating is mainly done by the sub-MeV electrons. It is found from Fig.5 (b), about 50% of core heating is done by the sub-MeV electrons, and the rest 50% is by the 1~10MeV electrons. Note that the reduction in the deposited energy for sub-MeV electron by inclusion of core hitting rate is pronounced since those low-energy electrons have large beam divergences and the core hitting rate is small for them.

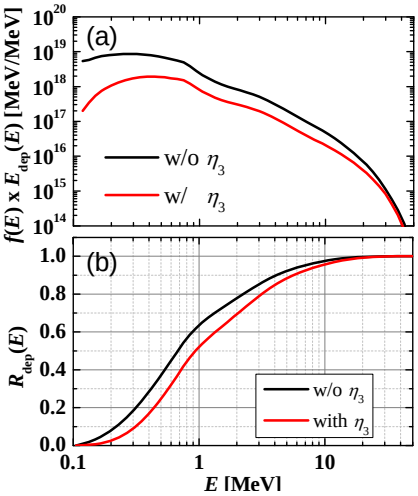

Fig.5 (a) Fast electron deposited energy and (b) contribution ratio for the case w/o pre-plasma case as a function of E.

The energy deposition rates integrated over fast electron energy, η_3, for the cases with and w/o pre-plasma, where the core hitting rate η_2 is not included, are η_3=32% and 12%, respectively. Three times larger value in the case w/o pre-plasma is due to the large number of electrons in the low energy region (E<10MeV).

4. SUMMARY

In the present paper, we evaluated the core heating performance for FIREX-I class experiments by separating the heating process into 3 phases; 1) energy coupling from heating laser to fast electrons η_1, 2) fast electron core hitting rate η_2 and 3) energy deposition rate in the core η_3. The obtained values and net coupling efficiencies η_{net} for the cases w/o and with pre-plasma are summarized in **Table I**. The existence of pre-plasma reduces the net coupling by 1/4. So reduction in pre-pulse level is indispensable for high heating efficiency. Another critical issue is the beam divergence. In the present analysis, the field effects such as self-guiding by resistive B-field are not included. When the beam divergence is as large as that obtained here, however, we cannot expect the self-guiding effect on beam transport [4] So we should find the methods for reduction in the beam divergence and / or additional beam-collimation method to enhance the heating efficiency. Otherwise, the tip should be as close to core as possible. The further investigations (e.g., more practical FP simulations for transport process, and double cone effects) are going on.

Table I Summary of core heating analysis

Pre-plasma	η_1 [%]	η_2 [%]	η_3 [%]	η_{net} [%]
w/o	72	36 (60)	32	8 (14)
with	45	34 (56)	12	1.8 (3)

A CD core (ρ=100g/cm^3 and R=20μm) is assumed for evaluation of η_2 and η_3. For η_2, Au tip with Δx_{tip} =5μm and D_{tip} = 50μm are assumed. The values in parentheses are for Au tip with Δx_{tip} =5μm and D_{tip} = 25μm case.

References

[1] H. Azechi, *et al.*, *Plasma Phys. Control. Fusion* **47** B267 (2006).
[2] R. Kodama, *et al.*, *Nature* **418** 933 (2002).
[3] Y. Yokota, *et al.*, *Phys. Plasmas* **13** 022702 (2006).
[4] C. Chen, et al, "*LLNL Fast Ignition Program*", presented at US-Japan Workshop on Fast Ignition and High Energy Density Physics, San Diego, CA, March 2010.